Electric field-induced monodomain blue phase liquid crystals

Yuan Chen and Shin-Tson Wu

Citation: Appl. Phys. Lett. **102**, 171110 (2013); doi: 10.1063/1.4803922
View online: http://dx.doi.org/10.1063/1.4803922
View Table of Contents: http://apl.aip.org/resource/1/APPLAB/v102/i17
Published by the American Institute of Physics.

Electric field-induced monodomain blue phase liquid crystals

Yuan Chen and Shin-Tson Wu[a)]
CREOL, The College of Optics and Photonics, University of Central Florida, Orlando, Florida 32816, USA

(Received 3 March 2013; accepted 17 April 2013; published online 1 May 2013)

We demonstrate an electric field-induced monodomain blue phase liquid crystal and its application for polarizer-free reflective displays. Superior to multidomain structure, the monodomain exhibits a relatively high reflectance and narrow bandwidth (~25 nm) so the reflected colors look vivid. As the applied voltage increases, the double-twist structure is gradually unwound so that Bragg reflection decreases leading to analogous grayscale. The submillisecond response time enables this reflective display to play videos without image blurs. Such a monodomain blue phase selectively reflects right-handed circularly polarized light when the employed chiral dopant is right-handed, and the reflected light is nearly circularly polarized. © *2013 AIP Publishing LLC*.
[http://dx.doi.org/10.1063/1.4803922]

Polymer-stabilized blue-phase liquid crystal (PS-BPLC)[1–5] exhibits several attractive features, such as submillisecond response time,[6,7] no need for surface alignment, and optical isotropy in the voltage-off state. It opens a gateway for high speed display and photonic applications.[8,9] Both transmissive and reflective BPLC devices have been demonstrated. In transmissive mode,[10,11] Bragg reflection is shifted to ultraviolet region by employing a high concentration chiral dopant so that it is optically isotropic in the visible spectral region. To realize amplitude modulation, the BPLC is sandwiched between two crossed polarizers. On the other hand, for reflective mode, the pitch length is adjusted to reflect colors in the visible region and no polarizer is needed. As a result, flexible display can also be realized.

Electrically tunable colors using BPLCs have been demonstrated based on the deformation of blue phase lattice.[12–14] However for polymer-stabilized blue phases, the cubic structures are stabilized by polymer network so that the lattice deformation can only take place in the high field region.[15] In the weak field region, the applied electric field mainly reorients the LC molecules. Recently, a vivid full-color reflective display using surface alignment-induced monodomain PS-BPLC has been demonstrated.[16] It exhibits relatively narrow reflection band, submillisecond response time, and voltage dependent analogous grayscales, while no polarizers and color filters are needed. However, the voltage is partially shielded by the surface alignment layer because of the large dielectric constant of the employed BPLC.[17] Besides reflective displays, monodomain blue phase has been used in photonics application, such as lasing,[18–20] where large area and uniform monodomain blue phase is critical.

In this letter, we demonstrate a large area vertical field-induced monodomain BPLC without any alignment layer. To distinguish from conventional multidomain structures, here, we refer to monodomain as having a poly-crystalline structure but with the same lattice orientation. The electric field is used to rotate the blue phase lattice and induce uniform texture.[21,22]

Blue phases appear between chiral-nematic phase and isotropic phase in a highly twisted chiral-nematic liquid crystal.[23] They exhibit self-assembled cubic structures and the local refractive index variation results in selective Bragg reflections. The reflection wavelength can be expressed as[24]

$$\lambda = \frac{2na}{\sqrt{h^2 + k^2 + l^2}}, \tag{1}$$

where n and a denote average refractive index and lattice constant of blue phases, and h, k, and l are the Miller indices of a crystal plane. When blue phase grows from isotropic phase without any electric field, multiple diffraction peaks can be observed from (110), (200), and (211) directions (with these lattice surfaces parallel to the substrate) of BP-I.[24] To generate narrow band reflection color, we applied a uniform electric field (E) perpendicular to the substrates to change the lattice orientation. The torque Γ exerted on the blue phase lattice of volume Ω can be described by[21]

$$\begin{aligned}\Gamma &= \Omega A \sum_{i=1}^{3} (n_i \cdot E)^3 (n_i \times E) \\ &= \Omega A[E_2E_3(E_2^2 - E_3^2)n_1 + E_1E_3(E_3^2 - E_1^2)n_2 \\ &\quad + E_1E_2(E_1^2 - E_2^2)n_3],\end{aligned} \tag{2}$$

where A is a proportional coefficient dependent on the material and n_i is the unit vector. When one of the following conditions is met, the torque will vanish: (1) $|E_1| = |E_2| = |E_3|$, i.e., E is normal to the (111) surface; (2) $E_i = E_j = 0$ and $|E_k| \neq 0$; i= 1, 2, 3; i≠ j ≠ k, i.e., E is normal to the (100) surface; and (3) $E_i = 0$ and $|E_j| = |E_k|$; i = 1, 2, 3; i ≠ j ≠ k, i.e., E is normal to the (110) surface. Thus, when the multidomain BP lattice is subject to an electric field, the nonzero torque will rotate the lattice to the nearest stable position where $\Gamma = 0$. To prove the concept, we prepared vertical field switching (VFS) cells, comprised of two ITO glass substrates but without polyimide alignment layer. The cell gap was controlled at 5 μm. The blue phase textures with and without electric effect are compared.

In the experiment, we used HTG-135200 (HCCH, China) as the nematic LC host. Its physical properties are

a)Electronic mail: swu@ucf.edu

listed as follows: $\Delta n = 0.205$ at $\lambda = 633$ nm, $\Delta\varepsilon = 99$ at 1 kHz, $\gamma_1 = 700$ mPa s at 25 °C, and clearing temperature $T_c = 98$ °C. To tune the reflection band from red to green and blue, we prepared BPLC mixtures with different concentrations of chiral dopant R5011 (HCCH). The chiral concentration is 3.46 wt. %, 3.94 wt. %, and 4.47 wt. % for the red, green, and blue cells, respectively. Afterwards, 10 wt. % of photocurable monomers [6 wt. % RM257 (Merck) + 4 wt. % TMPTA (1,1,1-Trimethylolpropane Triacrylate, Sigma Aldrich)] and 0.1 wt. % of photoinitiator were blended with 89.9 wt. % of the BPLC mixture to form the precursor. Next, we injected the LC/monomers mixture into a VFS cell and the cell was placed on a Linkam heating stage and cooled to blue phase. Different domains with different reflective colors appear, as shown in Figs. 1(a), 1(c), and 1(e). When the cell is subject to an AC electric field (1 kHz) of ~2 V/μm for about 1 s before UV curing, the toque created by the electric field helps to reorient the blue phase lattice. In our case, the (110) surface tends to align perpendicular to the electric field and the reflective color becomes uniform. Empirically, a smaller dielectric anisotropy and shorter pitch blue phase at a temperature closer to the chiral nematic phase requires a stronger electric field. As shown in Figs. 1(b), 1(d), and 1(f), monodomain blue phase is formed after the electric field pulse. Once the voltage is removed, the uniform BP texture remains unless it is heated up to an isotropic phase. These cells were then exposed to UV light ($\lambda = 365$ nm) with intensity of 6 mW/cm^2 for 10 min. After UV irradiation, polymer-stabilized BPLC nano-composites were self-assembled and the blue phase textures were stabilized.

To quantitatively compare the differences between multi-domain and monodomain blue phase cells, we measured their reflection spectra. A DH-2000 unpolarized light source (Mikropack) was coupled into a multi-mode fiber and incident on the PSBP cell normally. The reflected light was coupled back to the fiber and recorded by a high resolution spectrometer (HR2000 CG-UV-NIR, Ocean Optics). The reflection spectrum was normalized to that of a mirror. To avoid reflection from the glass and air surface, we attached an anti-reflection (AR) film to the front surface and a black tape to the back surface. Figure 1(g) depicts the measured reflection spectra of the green PSBP cell. Without electric field effect, the blue phase (Fig. 1(e)) shows a relatively low reflectance (black line). By contrast, the electric field-induced monodomain blue phase (Fig. 1(f)) exhibits a fairly high reflectance and narrow bandwidth (blue line). The peak reflectance (R_p) of the green cell is 35% at $\lambda = 527$ nm. The full width at half maximum (FWHM) of the reflection band is about 25 nm, so the appearance color is quite saturated and vivid. From here on, we will focus on the measured properties of electric field-induced monodomain blue phase.

The reflection spectra of red and blue cells were also measured [Figs. 2(a) and 2(c)]. Blue cell shows a reasonably high reflectance $R_p \sim 35.4\%$ at $\lambda \sim 472$ nm and FWHM ~ 21.4 nm. For the red cell, its peak reflectance ($R_p \sim 25.3\%$) occurs at $\lambda = 628$ nm and FWHM ~ 35.2 nm. The lower reflectance for the red cell is because Bragg reflection requires about ten pitch periods to establish. For a 5-μm cell gap, the red cell has fewer pitch periods because of its longer pitch. When an AC voltage is applied, the double-twist cylinders are

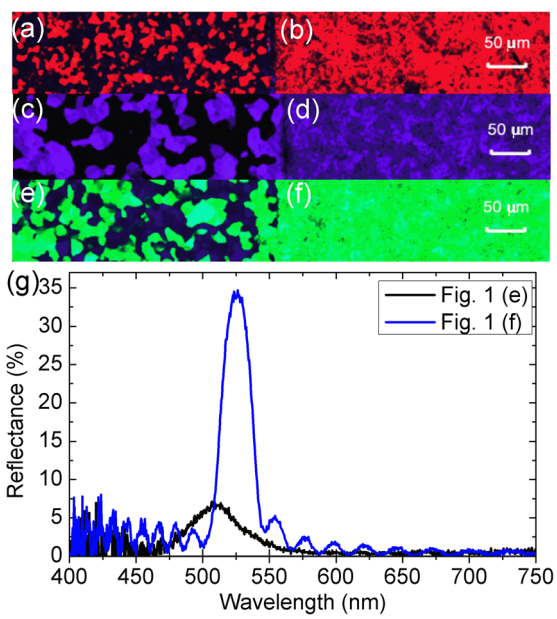

FIG. 1. Reflective microscope images of multi-domain BP for (a) red, (b) blue, and (c) green cells; monodomain BP for (b) red, (d) blue, and (f) green cells. Scale bar: 50 μm. (g) Measured reflection spectra of the green PSBP cell.

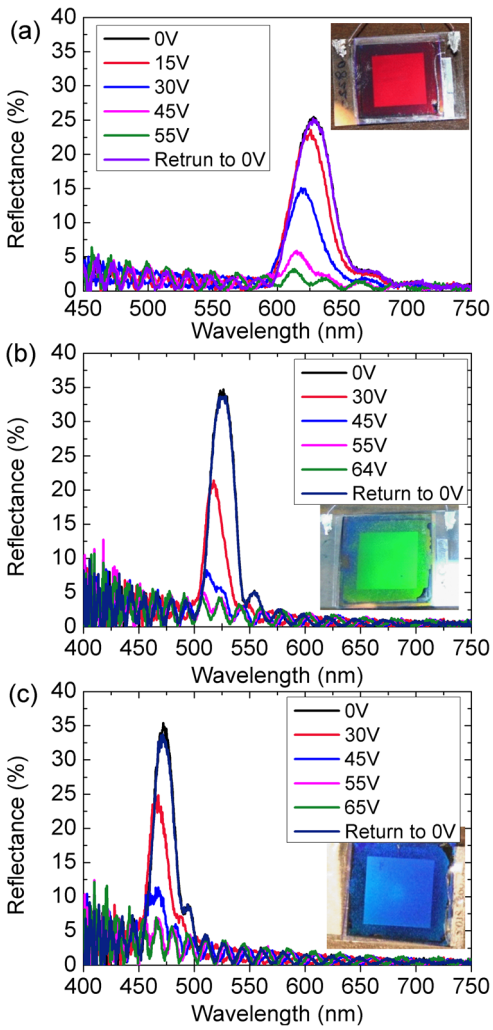

FIG. 2. Reflection spectra at different voltages for (a) red, (b) green, and (c) blue cells. The inset photos are the corresponding images at 0 V (ITO area in the center: 12 mm × 12 mm).

gradually unwound, which leads to a decreased reflectance. Figure 2 depicts the reflection spectra at different operating voltages for the red, green, and blue cells. Analogous gray-scale can be controlled by the applied voltage. A tiny blue shift (<5 nm) on the peak reflection wavelength is observed, indicating the lattice deformation of the PS-BPLC is very minor. The refection drops to baseline as the voltage keeps increasing. This is because the LC molecules have been reoriented by the electric field. The reflectance (R_0) at a high voltage gives the dark state. The contrast ratio (CR) is defined as R_p/R_0. To improve CR, we should minimize R_0, which is governed by the reflections of the ITO/PSBP and ITO/glass interfaces. A more noticeable R_0 is found for the blue BPLC cell because of the increased index mismatch between the ITO/PSBP and ITO/glass. The calculated CR is 9.4:1 at 65 V, 14.9:1 at 64 V, and 16.6:1 at 55 V for the blue, green, and red cells, respectively. The CR can also be improved with the index-matched electrode. To reduce operation voltage, a BPLC with a larger Kerr constant can be considered.[25–27]

The properties of reflected light from the PSBP cells are also studied. The inset plots in the Fig. 3 show the reflected beam pattern from a red cell (right) and a green cell (left), for example. A He-Ne laser beam was used as a probing beam for the red cell and an Argon laser beam ($\lambda = 514$ nm) for the green cell, respectively. The incident angle was kept small (<5°). The intensity distribution of the reflection pattern is quite symmetric, and the FWHM angle is about 8° for the red cell, based on the angular intensity distribution plotted in Fig. 3. This phenomenon happens to the blue and green cells as well, but with a smaller spreading angle. For the green cell, the reflective beam size is more collimated compared to the red cell, as shown in Fig. 3. The FWHM angle is estimated to be 2.4°. Unlike the surface alignment-induced monodomain blue phase which exhibits a specular reflection as a mirror does, the electric field-induced monodomain blue phase is slightly diffusive. Before UV stabilization, the short electric field pulse helps to rotate the BP lattice and align (110) surface parallel to the substrate. When the electric field is released, some of the (110) planes tend to relax back to the original state to some extent, but there is insufficient energy for these lattices to relax back because of the high viscosity of BP,[24] resulting in some slightly tilted planes and hence the diffusive reflected beam. In the red cell, the viscosity is smaller due to the lower chiral dopant concentration and higher BP temperature range than that of the green and blue cells. Thus, the BP lattice of the red cell has freedom to rotate more, leading to a larger spreading angle in the reflected beam. This intrinsic diffusive reflection also helps to widen the viewing angle.

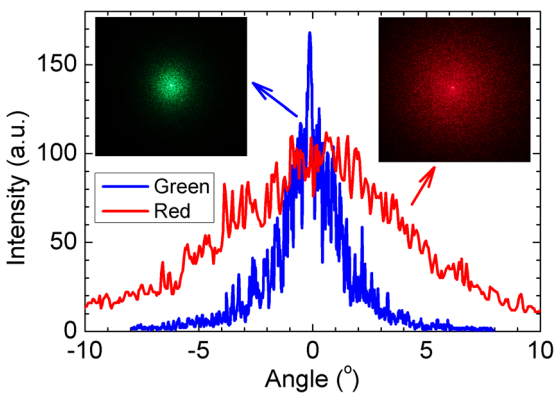

FIG. 3. Angular intensity distribution of the reflected beam from the red and green PBLC cell (Incident light: He-Ne laser beam for red cell and Argon laser beam for the green cell). Inset plots show the beam patterns.

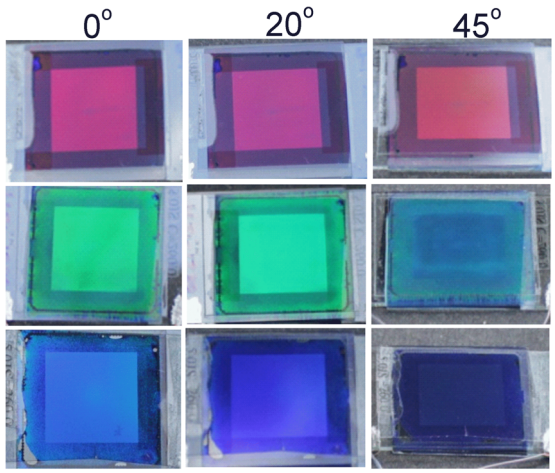

FIG. 4. Outdoor viewing angle performance of the R, G, and B cells.

To study the viewing angle performance of the cells, we did an outdoor experiment and took pictures of the red, green, and blue cells at different viewing angles, as Fig. 4 shows. When viewing at normal direction (0°), we can observe vivid colors for all the red, green, and blue cells. The actual color appears more saturated when viewing with eyes, as the CCD camera tends to degrade the color quality. At 20°, we can still see vivid colors but the blue shift is gradually taking place, since blue phase has well organized photonic crystalline structure and has intrinsic angular dependent reflection wavelength. The blue shift becomes more evident as the viewing angle increases to ~45°, which is consistent with those results reported previously.[28]

The voltage-dependent reflectance (VR) curve and the response time were measured using a He-Ne laser for the red cell as an example. Based on the above mentioned property, the reflected beam is divergent and a portion of the light is not coupled back into the fiber and the spectrometer. Therefore, a lens is inserted between the PSBP cell and the photodiode detector (New Focus Model 2031) to collect most of the reflected light. A 1-kHz square-wave AC signal was applied to the VFS cell, and the corresponding reflectance was recorded by a LABVIEW system. For a linearly polarized (LP) incident light, the reflectance is 34.4% at 0 V and drops to 1.4% at 56 V, shown as the black line in Fig. 5. The dark state light leakage comes from the reflection of the ITO/PSBP and ITO/glass interfaces. The CR is about 24.8:1 at $\lambda = 633$ nm. A $\lambda/4$ plate was inserted to change the polarization state of the incident light. For the right-handed circularly polarized (RCP) light, the reflectance is 65.4%, which is almost doubled compared to the LP incident light. On the contrary, the reflectance is only 3.2% (red dot in Fig. 5) when the incident light is left-handed circularly polarized (LCP). The chiral dopant used in our PSBP system is right handed, so only the RCP will be reflected. For a PSBP system with left-hand chiral dopant, only LCP light will be reflected. This

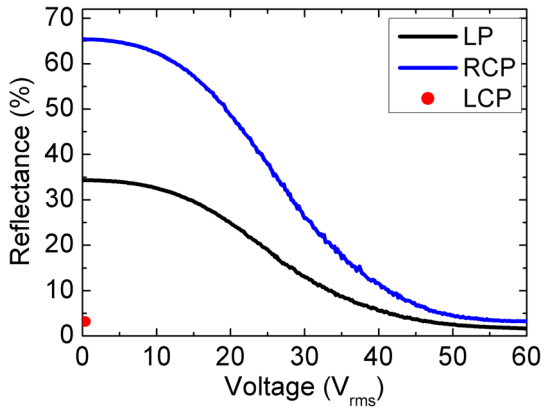

FIG. 5. Measured VR curves for LP and RCP incident lights, and reflectance for LCP at 0 V.

polarization selectivity in the reflection makes this device promising for many photonic and display devices.

Fast response time is one of the most attractive features for BPLC. Both rise time and decay time were measured between 10% and 90% transmittance change. The measured decay time (56 V-0 V) at room temperature is 814 μs and rise time (0 V-56 V) is 64 μs. Such a fast response time enables video-rate operation of the reflective display without image blurring.

There have been some arguments about the polarization state of the reflected light of blue phase liquid crystals.[16,19,29–31] Here, we experimentally investigated the polarization state with a $\lambda/4$ plate and a linear polarizer inserted before the detector. The reflected light is right-handed for both RCP and LP incident beams. We rotated the linear polarizer in front of the detector in step of 10° and recorded the light intensity. Figure 6 shows the polarization ellipse of the reflected light for both RCP and LP incident lights. The ellipticity ε is defined as the ratio of the major axis to the minor axis of the polarization ellipse. $\varepsilon = 0$ or ∞ represents LP and $\varepsilon = 1$ means circular polarization. The measured ε of the reflected light is 0.985 and 0.991 for the RCP and LP incident lights, respectively, indicating the reflected light is

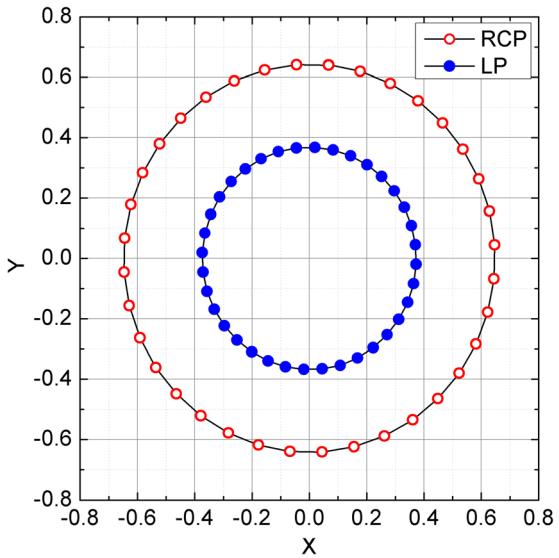

FIG. 6. Polarization state of the reflected light for RCP (open circle) and LP (solid circle) incident beams.

very close to circularly polarized, regardless of the polarization state of the incident light. Unlike the surface alignment induced monodomain BP,[16] the alignment layers can also affect the LC molecular orientation which would further affect the polarization state and resulting in a lower ε of 0.68.

In summary, we have demonstrated an electric field-induced monodomain blue phase and its application for reflective displays. The reflection spectra for red, green, and blue cells were studied. The bandwidth is fairly narrow so the color looks saturated and vivid. The reflectance gradually decreases with the increasing operating voltage and analogous grayscales can be achieved. With analog grayscales and submillisecond response time, videos can be displayed using this reflective PSBP. Moreover, the electric-field-induced monodomain blue phase selectively only reflects RCP light when the employed chiral dopant is right-handed, and the reflected light is almost circularly polarized.

The authors are indebted to Zhenyue Luo and Jin Yan for helpful discussion and Industrial Technology Research Institute (ITRI, Taiwan) for financial support.

[1]H. Kikuchi, M. Yokota, Y. Hisakado, H. Yang, and T. Kajiyama, Nature Mater. **1**, 64 (2002).
[2]Y. Hisakado, H. Kikuchi, T. Nagamura, and T. Kajiyama, Adv. Mater. **17**, 96 (2005).
[3]J. Yan, L. Rao, M. Jiao, Y. Li, H. Cheng, and S. T. Wu, J. Mater. Chem. **21**, 7870 (2011).
[4]Z. Ge, S. Gauza, M. Jiao, H. Xianyu, and S. T. Wu, Appl. Phys. Lett. **94**, 101104 (2009).
[5]L. Rao, S. He, and S. T. Wu, J. Disp. Technol. **8**, 555 (2012).
[6]K. M. Chen, S. Gauza, H. Xianyu, and S. T. Wu, J. Disp. Technol. **6**, 49 (2010).
[7]Y. Chen, J. Yan, J. Sun, S. T. Wu, X. Liang, S. H. Liu, P. J. Hsieh, K. L. Cheng, and J. W. Shiu, Appl. Phys. Lett. **99**, 201105 (2011).
[8]Y. H. Lin, H. S. Chen, H. C. Lin, Y. S. Tsou, H. K. Hsu, and W. Y. Li, Appl. Phys. Lett. **96**, 113505 (2010).
[9]J. Yan, Y. Li, and S. T. Wu, Opt. Lett. **36**, 1404 (2011).
[10]L. Rao, Z. Ge, S. T. Wu, and S. H. Lee, Appl. Phys. Lett. **95**, 231101 (2009).
[11]H. C. Cheng, J. Yan, T. Ishinabe, and S. T. Wu, Appl. Phys. Lett. **98**, 261102 (2011).
[12]H. S. Kitzerow, Mol. Cryst. Liq. Cryst. **202**, 51 (1991).
[13]G. Heppke, M. Krumrey, and F. Oestreicher, Mol. Cryst. Liq. Cryst. **99**, 99 (1983).
[14]C. T. Wang, H. Y. Liu, H. H. Cheng, and T. H. Lin, Appl. Phys. Lett. **96**, 041106 (2010).
[15]S. Y. Lu and L. C. Chien, Opt. Lett. **35**, 562 (2010).
[16]J. Yan, S. T. Wu, K. L. Cheng, and J. W. Shiu, Appl. Phys. Lett. **102**, 081102 (2013).
[17]M. Jiao, Z. Ge, Q. Song, and S. T. Wu, Appl. Phys. Lett. **92**, 061102 (2008).
[18]W. Y. Cao, A. Munoz, P. Palffy-Muhoray, and B. Taheri, Nature Mater. **1**, 111 (2002).
[19]S. Yokoyama, S. Mashiko, H. Kikuchi, K. Uchida, and T. Nagamura, Adv. Mater. **18**, 48 (2006).
[20]H. J. Coles and S. Morris, Nat. Photonics **4**, 676 (2010).
[21]P. Pieranski, P. E. Cladis, T. Garel, and R. Barbetmassin, J. Phys. **47**, 139 (1986).
[22]K. Uchida, Y. Hisakado, H. Kikuchi, and T. Kajiyama, Trans. Mater. Res. Soc. Jpn. **29**, 819 (2004).
[23]H. S. Kitzerow and C. Bahr, *Chirality in Liquid Crystals* (Springer, New York, 2001).
[24]H. Kikuchi, *Liquid Crystalline Blue Phases* (Springer, Berlin, 2008).
[25]L. Rao, J. Yan, S. T. Wu, S. Yamamoto, and Y. Haseba, Appl. Phys. Lett. **98**, 081109 (2011).
[26]M. Wittek, N. Tanaka, D. Wilkes, M. Bremer, D. Pauluth, J. Canisius, A. Yeh, R. Yan, K. Skjonnemand, and M. Klasen-Memmer, SID Int. Symp. Digest Tech. Papers **43**, 25 (2012).

[27]Y. Chen, D. Xu, S. T. Wu, S. Yamamoto, and Y. Haseba, Appl. Phys. Lett. **102**, 141116 (2013).
[28]J. H. Flack and P. P. Crooker, Mol. Cryst. Liq. Cryst. **69**, 281 (1981).
[29]R. M. Hornreich and S. Shtrikman, Phys. Rev. A **28**, 1791 (1983).
[30]C. Bohley and T. Scharf, J. Opt. A, Pure Appl. Opt. **6**, S77 (2004).
[31]F. Castles, F. V. Day, S. M. Morris, D. H. Ko, D. J. Gardiner, M. M. Qasim, S. Nosheen, P. J. W. Hands, S. S. Choi, R. H. Friend, and H. J. Coles, Nature Mater. **11**, 599 (2012).